2-1-1992

Hamiltonian bifurcation theory of closed orbits in the diamagnetic Kepler problem

J. M. Mao

J. B. Delos

Hamiltonian bifurcation theory of closed orbits in the diamagnetic Kepler problem

J.-M. Mao and J. B. Delos
Department of Physics, College of William & Mary, Williamsburg, Virginia 23185
(Received 18 April 1991)

Classically chaotic systems possess a proliferation of periodic orbits. This phenomenon was observed in a quantum system through measurements of the absorption spectrum of a hydrogen atom in a magnetic field. This paper gives a theoretical interpretation of the bifurcations of periodic or closed orbits of electrons in atoms in magnetic fields. We ask how new periodic orbits can be created out of existing ones or "out of nowhere" as the energy changes. Hamiltonian bifurcation theory provides the answer: it asserts the existence of just five typical types of bifurcation in conservative systems with two degrees of freedom. We show an example of each type. Every case we have examined falls into one of the patterns described by the theory.

PACS number(s): 32.60.+i, 32.80.−t, 05.45.+b

I. INTRODUCTION

If an atom is placed in an external electric or magnetic field and the photoabsorption spectrum is measured at finite resolution, then the absorption cross section as a function of photon energy consists of a smooth background plus a superposition of sinusoidal oscillations (quasi-Landau oscillations, or Garton-Tomkins-Edmonds effect). Each oscillation is correlated with a closed classical orbit of the electron as it moves under the Coulomb force of the residual ion and the external electric or magnetic fields [1,2].

An especially precise method for observing these oscillatory spectra was developed by Holle *et al.* [3]. For an atom in a magnetic field, it was known that the shape of any classical orbit depends only on the scaled energy $\varepsilon = E/B^{2/3}$, and that at fixed scaled energy, the action on that orbit varies with magnetic field as $B^{-1/3}$. Therefore, by measuring the photoabsorption cross section at fixed scaled energy (varying the photon energy and the magnetic-field strength simultaneously), they were able to measure the oscillations with high precision, and to observe the change of the oscillations with changing scaled energy. Their results are shown in Fig. 2 of Ref. [3(b)].

The most striking phenomenon that is visible in that picture is the proliferation of closed classical orbits as the energy increases. This proliferation is correlated with a qualitative change in the classical dynamics of the electron: at low energy orbits are regular, while at high energies they are chaotic. It has been known since the work of Poincaré and Birkhoff that regular classical systems possess limited, orderly sequences of periodic orbits, while chaotic systems show a proliferation of periodic orbits [4]. The measurements of Holle and co-workers constitute the first direct observation of this phenomenon in an atomic system. The measurements have additional interest because the atom actually obeys laws of quantum mechanics, so the observations also give new information about the relationship between quantum and classical mechanics.

This is one of a set of papers [5] that examine the theory of periodic orbits and of closed orbits, and that compare the results of theory with observations. In examining the experimental results and thinking about the classical transition from order to chaos, one may be reminded of the sequence of period-doubling bifurcations occurring in one-dimensional maps. Through the work of Metropolis, Stein, and Stein, Feigenbaum, Collet and Eckmann, and others, both the local structure of individual bifurcations and the global structure of the sequence of bifurcations is now well understood [6,7]. Unfortunately, little of that knowledge is directly applicable here. The behavior of the diamagnetic Kepler system is governed not by a one-dimensional unimodal map, but rather by a two-dimensional area-preserving map. And even though Feigenbaum-type sequences have been unearthed and analyzed for such maps, we find that such sequences are not prominent in the Bielefeld measurements. What is the theoretical framework for interpreting the observations?

In this paper and future ones, we will show that bifurcation theory for Hamiltonian systems provides such a framework. The theory asserts that in two-dimensional area-preserving maps (corresponding to conservative systems with two degrees of freedom) there are five and only five typical types of bifurcation [8]. Some of these five types may be modified by special symmetries of the system. We have examined a large number of bifurcations of periodic orbits in the diamagnetic Kepler system, and we have seen examples of every type. More important, every bifurcation we have seen fits into one of the classes described by the theory.

The paper is organized as follows. In Sec. II, notation is given, the Hamiltonian is specified, and a relationship is established between closed orbits of the electron and periodic points of a map. To take advantage of the symmetries of the system, the Poincaré map is defined in an unusual way.

In Sec. III and the Appendices, we review present knowledge about Hamiltonian bifurcation theory. The five typical bifurcations are described.

Then in Secs. IV–VII we present a series of case stud-

ies, illustrating the structure of each bifurcation. The reader who wearies of the details of each case may at any time go to the summary in Sec. VIII. The demonstration that these bifurcations are visible in experiments is left to a future paper.

Keeping these successes of the theory in mind, let us also mention a significant limitation of current knowledge of Hamiltonian bifurcation theory. As presently formulated, it is said to be a *local* theory, but not a *global* one. This means that it describes the local structure of each bifurcation *in a sufficiently small region* of phase space and parameter space. To get a global picture, one must tie together all of the local pictures in each region.

It is evident that the local description is very important: first, it does give an interpretation of observations, and second, any global theory of sequences of bifurcations must begin from a local theory. However, it is also helpful to bear in mind that the general theory of bifurcations of two-dimensional maps does not yet make any predictions about *sequences* of bifurcations that are useful in the present context. We hope to report some advances on this problem in the future.

II. FUNDAMENTALS

A. Hamiltonian

The Hamiltonian of a hydrogenic electron (in a state with magnetic quantum number equal to zero) in a uniform magnetic field **B** directed along the z axis is given by

$$H=(1/2m)(p_\rho^2+p_z^2)-e^2/(\rho^2+z^2)^{1/2}+\tfrac{1}{8}m\omega_c^2\rho^2 , \quad (2.1)$$

where $\omega_c=eB/mc$ is the cyclotron frequency. Here we use cylindrical coordinates (ρ,z,ϕ), and the ϕ motion has been separated. Converting to atomic units and using the scaled variables [9]

$$\mathbf{r}=\tfrac{1}{2}\gamma^{2/3}\mathbf{r}, \quad \gamma=B/c, \quad \mathbf{p}=\gamma^{-1/3}\mathbf{p} , \quad (2.2)$$

the Hamiltonian becomes

$$H=\tfrac{1}{2}[p_\rho^2+p_z^2-1/(\rho^2+z^2)^{1/2}+\rho^2] . \quad (2.3)$$

The parameter γ, which is written as B/c in atomic units, can be expressed more fully as B/B_0, where $B_0=m^2e^3c/\hbar^3=2.35\times10^5$ T. We further transform the coordinates to semiparabolic coordinates [10] (u,v,τ),

$$\begin{aligned} z&=u^2-v^2 , \\ \rho&=2uv , \\ \frac{d\tau}{dt}&=\frac{1}{4r(t)} , \end{aligned} \quad (2.4)$$

to obtain the form of the Hamiltonian that will be used through the rest of this paper:

$$h=\tfrac{1}{2}(p_u^2+p_v^2)-4\varepsilon(u^2+v^2)+8u^2v^2(u^2+v^2)=2 , \quad (2.5)$$

where $\varepsilon=E\gamma^{-2/3}$ is called the scaled energy. The new Hamiltonian depends upon just this one parameter, ε.

The coordinate transformation (2.4) maps the half-plane $(0\le\rho\le\infty, \ -\infty<z<\infty)$ into the quarter plane $(0\le u<\infty, \ 0\le v<\infty)$. (The positive z axis corresponds to $v=0$, the negative z axis corresponds to $u=0$, and the ρ axis becomes the line $u=v$.) In principle, any orbit that approaches the u or v axis should be reflected at the axis such that it stays in the positive quadrant. However, in computing and drawing orbits in (u,v) space, it is easier to permit the orbits to pass through the axes. The orbits then possess certain symmetries.

B. Symmetries

The Hamiltonian (2.5) is an even function of each coordinate and each momentum. As a consequence, given any section of an orbit, that section can be reflected through the u axis or through the v axis, and it is then a section of another orbit (Fig. 1).

This symmetry is expressed analytically in the following way. Let us represent an orbit as a function of (scaled) time τ and of the initial conditions: $u=u(\tau;u^0,p_u^0,v^0,p_v^0)$, etc. Then, given any orbit, there always exists a second, usually distinct orbit, which is the reflection of the orbit through the v axis:

$$\begin{aligned} u(\tau;u^0,p_u^0,-v^0,-p_v^0)&=+u(\tau;u^0,p_u^0,v^0,p_v^0) , \\ v(\tau;u^0,p_u^0,-v^0,-p_v^0)&=-v(\tau;u^0,p_u^0,v^0,p_v^0) , \\ p_u(\tau;u^0,p_u^0,-v^0,-p_v^0)&=+p_u(\tau;u^0,p_u^0,v^0,p_v^0) , \\ p_v(\tau;u^0,p_u^0,-v^0,-p_v^0)&=-p_v(\tau;u^0,p_u^0,v^0,p_v^0) , \end{aligned} \quad (2.6)$$

a third orbit, which is the corresponding reflection through the u axis, and a fourth, which is the reflection through both axes. The Hamiltonian is also symmetric under reflection through the line $u=\pm v$, and so the orbits have symmetries analogous to (2.6) for reflection through these lines.

Experiments give a signal (a peak in the Fourier transform of the absorption spectrum) for all closed orbits in ρz space that start and end at the nucleus. For every orbit in ρz space that is closed at the nucleus and has return time T_c, there is a periodic orbit in uv space that passes through the origin and has period $T=2T_c$. Each periodic orbit consists of two closed orbits that are identical ex-

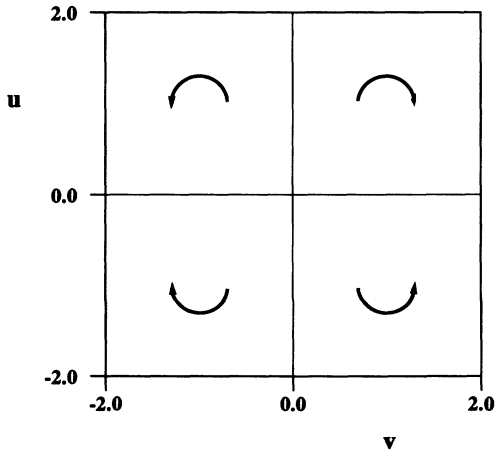

FIG. 1. Sections of orbits illustrating the symmetries, cf. Eqs. (2.6) and (3.8).

cept for orientation. In this paper we discuss those periodic orbits in uv space. In comparing with experiment we note that the signal associated with such an orbit appears at $T_c = T/2$, and the properties of the signal are related to properties of one-half cycle of that orbit.

We note that other periodic orbits also exist that do not pass through the origin. They will not be considered here, except for a few that pass close to the origin, and which are involved in bifurcation of the periodic orbits.

C. A Poincaré map

For $\varepsilon < 0$, every orbit passes through $u = 0$ at least once. For $\varepsilon > 0$, we are still mainly concerned with orbits that pass through the origin, so these orbits certainly pass through $u = 0$. When $u = 0$, v can have any value such that $-4\varepsilon v^2 \leq 2$, and p_v can have any value such that $\frac{1}{2}p_v^2 - 4\varepsilon v^2 \leq 2$. Then p_u is determined from Eq. (2.5) together with the convention $p_u \geq 0$. With these values of uvp_up_v as initial conditions, Hamilton's equations of motion can be integrated forward in time until u again passes through zero with p_u positive, and the resulting values of v and p_v, can be recorded. This procedure defines the conventional Poincaré map.

In this paper, it is better to define a different Poincaré map. Starting as before, the equations are integrated forward in time until u passes through zero with *either sign* of p_u, and the values of v ad p_v are recorded. This defines what we sometimes call the "half"-Poincaré map to distinguish it from the conventional or "full" Poincaré map. Because of the symmetry on reflection through the u axis [analogous to (2.6)], this Poincaré map is well defined, one to one, area preserving, and indeed, has all the properties of conventional Poincaré maps.

Henceforth we denote

$$p_v \equiv p, \quad v \equiv q \ , \tag{2.7}$$

the pair of variables (p,q) is denoted

$$\mathbf{z} \equiv (p,q) \ , \tag{2.8}$$

and the mapping is abbreviated

$$\mathbf{z}_1 = \mathbf{f}(\mathbf{z}_0;\varepsilon) \ . \tag{2.9}$$

Associated with the map is the Jacobian matrix

$$\underline{J}_1(\mathbf{z};\varepsilon) \equiv \begin{bmatrix} \dfrac{\partial p_1(p,q;\varepsilon)}{\partial p} & \dfrac{\partial p_1(p,q;\varepsilon)}{\partial q} \\ \dfrac{\partial q_1(p,q;\varepsilon)}{\partial p} & \dfrac{\partial q_1(p,q;\varepsilon)}{\partial q} \end{bmatrix} . \tag{2.10}$$

The determinant of this matrix is everywhere equal to 1 (area preservation), and its trace is denoted

$$\mathrm{Tr}_1(\mathbf{z};\varepsilon) \equiv \mathrm{Tr}[\underline{J}_1(\mathbf{z};\varepsilon)] \ . \tag{2.11}$$

Starting from any point $\mathbf{z}$, the map can be iterated k times, so that

$$\begin{aligned} \mathbf{z}_1 &= \mathbf{f}(\mathbf{z};\varepsilon) \ , \\ \mathbf{z}_2 &= \mathbf{f}(\mathbf{z}_1;\varepsilon) \ , \\ &\cdots \\ \mathbf{z}_k &= \mathbf{f}(\mathbf{z}_{k-1};\varepsilon) \ . \end{aligned} \tag{2.12}$$

The kth iterate of the map, $\mathbf{z}' = \mathbf{f}^{(k)}(\mathbf{z};\varepsilon)$ is called the k map, the Jacobian matrix for this iterated map is denoted

$$\underline{J}_k(\mathbf{z};\varepsilon) \equiv \begin{bmatrix} \dfrac{\partial p_k(p,q;\varepsilon)}{\partial p} & \dfrac{\partial p_k(p,q;\varepsilon)}{\partial q} \\ \dfrac{\partial q_k(p,q;\varepsilon)}{\partial p} & \dfrac{\partial q_k(p,q;\varepsilon)}{\partial q} \end{bmatrix} , \tag{2.13}$$

and its trace is denoted

$$\mathrm{Tr}_k(\mathbf{z};\varepsilon) = \mathrm{Tr}[\underline{J}_k(\mathbf{z};\varepsilon)] \ . \tag{2.14a}$$

It is not hard to show that the trace of $\underline{J}_k$ is related to the trace of $\underline{J}_1$ by the formula

$$\mathrm{Tr}_k(\mathbf{z};\varepsilon) = 2\cos\{k\cos^{-1}[\mathrm{Tr}_1(\mathbf{z};\varepsilon)/2]\} \tag{2.14b}$$

for $|\mathrm{Tr}_1(\mathbf{z};\varepsilon)| < 2$. For $|\mathrm{Tr}_1(\mathbf{z};\varepsilon)| > 2$, the cos's are replaced by cosh's.

An m-periodic orbit of the map is the set of points $(\mathbf{z}_0,\mathbf{z}_1,\mathbf{z}_2,\ldots,\mathbf{z}_m,\ldots)$ generated according to (2.12) such that the mth iteration returns to the initial point:

$$\mathbf{z}_m = \mathbf{z}_0 \ . \tag{2.15}$$

Since Poincaré maps are originally defined through solutions to Hamilton's equations, normally each periodic orbit of the map $(\mathbf{z}_0,\mathbf{z}_1,\mathbf{z}_2,\ldots)$ corresponds to a periodic orbit of the differential equations $[u(\tau),v(\tau),p_u(\tau),p_u(\tau)$, with $u(T) = u(0)$, etc.]. However, because of our unconventional definition of the map, each periodic orbit of the map corresponds either to a periodic orbit or to a closed orbit of the dynamical system. Orbits pass through $u = 0$ with p_u alternating positive and negative on each pass, so an odd-m-periodic orbit of the map is a closed orbit of the system—it is half of a periodic orbit of twice the length. Even-m-periodic orbits of the map are periodic orbits of the system.

The traces $\mathrm{Tr}_1(\mathbf{z}_0;\varepsilon)$ and $\mathrm{Tr}_m(\mathbf{z}_0;\varepsilon)$ evaluated at the initial point of a periodic orbit play a fundamental role in the stability and bifurcation theorems given below.

III. HAMILTONIAN BIFURCATION THEORY

General theories about the existence, structure, and bifurcations of periodic orbits of dynamical systems are still under development. There are many references on this subject [11], some of which are quite detailed, rigorous, and incomprehensible. However, for conservative systems having only two degrees of freedom, there are important simple and general theorems, which have been obtained by Meyer and extended by de Aguiar *et al.* [8]. Meyer's theorems list and describe the bifurcations that occur in "typical" two-dimensional area-preserving maps. Our system has symmetries that make it "atypical" in certain ways. Therefore, we will first review

Meyer's results, and then summarize the modifications of those results that arise from the symmetries.

In this section we consistently discuss periodic orbits of the Poincaré half-map. As explained earlier, each corresponds either to a periodic or to a closed orbit of the Hamiltonian system.

A. General theorems

(1) *Stability of an m-periodic orbit.* We presume that at some value of ε, and some $\mathbf{z}_0$ there is an m-periodic orbit. If the absolute value of the trace $\mathrm{Tr}_m(\mathbf{z}_0;\varepsilon)$ is less than 2 (respectively greater than 2), then at that ε the periodic orbit beginning at $\mathbf{z}_0$ is stable (respectively unstable):

$$\begin{aligned} &|\mathrm{Tr}_m(\mathbf{z}_0;\varepsilon)|<2\rightarrow\text{stable}\ , \\ &|\mathrm{Tr}_m(\mathbf{z}_0;\varepsilon)|>2\rightarrow\text{unstable}\ . \end{aligned} \tag{3.1a}$$

For the unstable case, the Lyapunov exponent λ is related to the trace by

$$\lambda=\cosh^{-1}[\mathrm{Tr}_m(\mathbf{z}_0;\varepsilon)/2]\ . \tag{3.1b}$$

In the stable case, the quantity

$$\omega=\cos^{-1}[\mathrm{Tr}_m(\mathbf{z}_0;\varepsilon)/2] \tag{3.1c}$$

represents the winding rate of the neighbors around the periodic orbit [7].

(2) *Persistence of periodic orbits.* We presume that the dynamical system and its associated Poincaré map are well defined and smooth in an open domain of phase space and parameter space. Inside this region, at some value $\varepsilon=\varepsilon_0$, there is an m-periodic orbit $(\mathbf{z}_0,\mathbf{z}_1,\ldots,\mathbf{z}_{m-1},\mathbf{z}_m=\mathbf{z}_0,\ldots)$. If $\mathrm{Tr}_m(\mathbf{z}_0;\varepsilon)$ is not equal to 2, then that periodic orbit is a member of a smooth one-parameter family of m-periodic orbits $(\mathbf{z}_0(\varepsilon),\mathbf{z}_1(\varepsilon),\ldots,\mathbf{z}_m(\varepsilon)=\mathbf{z}_0(\varepsilon),\ldots)$ that exists over an interval of ε containing ε_0. Less formally stated, the orbit continues to exist over a range of the parameter, and its precise shape is a continuous function of the parameter.

The converse is the important statement: periodic orbits cannot appear and disappear capriciously. Inside of an open domain, a new m-periodic orbit can appear or an existing m-periodic orbit can disappear only at points $(\mathbf{z}_0,\varepsilon_0)$ such that

$$\mathrm{Tr}_m(\mathbf{z}_0;\varepsilon)=2\ . \tag{3.2}$$

Such points are called m-bifurcation points.

This theorem strictly limits the possible bifurcations of orbits. For example, it asserts that an isolated periodic orbit with a positive-definite Lyapunov exponent cannot bifurcate. However, outside of the conditions of this theorem, there are two other ways that periodic orbits can appear and disappear: (1) If the mapping ceases to exist at some value of the parameter, then obviously all of its orbits disappear [12]. (2) If the mapping is defined on a finite, closed space, then orbits can appear and disappear at the boundary. This theorem makes no assertion about such cases.

The following theorem also deals only with bifurcations that occur in the interior of a region of phase space and parameter space. This good news provides the conceptual framework for this paper:

(3) *There are five and only five typical types of bifurcations of two-dimensional area-preserving maps:* one each for $m=1,2,3,4$ and one for $m\geq 5$. Common names for these bifurcations are

m	Names
1	Saddle-node bifurcation
2	Period-doubling bifurcation
3	"Touch-and-go" bifurcation
4	"Touch-and-go" or four-island chain bifurcation
≥ 5	Five-island chain or m-island chain bifurcation

(3.3)

Properties of each of these bifurcations are discussed in Appendix A.

(4) *Location of m-bifurcation.* Consider an existing orbit, $\mathbf{z}_0(\varepsilon)$, of period one. The Jacobian matrix evaluated at this orbit, $\underline{J}_1(\mathbf{z}_0(\varepsilon),\varepsilon)$, depends on the parameter. When the trace of the mth power of this Jacobian matrix reaches 2, the m-bifurcation occurs,

$$\mathrm{Tr}_m(\mathbf{z}_0(\varepsilon_m);\varepsilon_m)=\mathrm{Tr}\{[\underline{J}_1(\mathbf{z}_0(\varepsilon_m);\varepsilon_m)]^m\}=2\ , \qquad m=1,2,\ldots \tag{3.4}$$

where ε_m is the critical value of the parameter ε for the m-bifurcation. Equivalently, the m-bifurcation occurs when

$$\begin{aligned} &\mathrm{Tr}_1(\mathbf{z}_0(\varepsilon_m);\varepsilon_m)=2\cos(2\pi j/m)\ , \\ &\quad j=1 \ \text{ if } m\leq 4 \\ &\quad j=1,2 \ \text{ if } m=5 \\ &\quad \cdots\ . \end{aligned} \tag{3.5}$$

Explicitly, these conditions for bifurcation are

$$\mathrm{Tr}_1(\mathbf{z}_0(\varepsilon_m);\varepsilon_m)=\begin{cases} 2, & m=1 \\ -2, & m=2 \\ -1, & m=3 \\ 0, & m=4 \\ (\sqrt{5}-1)/2 \ \text{ or } \ -(\sqrt{5}+1)/2, & m=5 \\ \cdots\ . \end{cases} \tag{3.6}$$

Hence by plotting $\mathrm{Tr}_1(\mathbf{z}_0(\varepsilon);\varepsilon)$ as a function of ε, we can locate the values ε_m at which the m-bifurcation occurs.

B. Bifurcations of antisymmetric maps

Meyer's theorem lists the "typical" bifurcations of periodic orbits of maps. The word "typical" has the same meaning that it has in catastrophe theory [13]: other types of bifurcation are possible, but they are unusual. To understand the meaning of this, consider a function $f(x)$ which has an extremum at a point x^*. The "typical" extremum is a quadratic one, $f(x)=f(x^*)$

$+\frac{1}{2}f''(x^*)(x-x^*)^2+\ldots$. Only for "unusual" functions does $f''(x)$ vanish at the same point at which $f'(x)$ vanishes [14].

A closely related argument was used by Meyer to show that the only typical bifurcations of periodic orbits are the ones listed. The argument is based upon Taylor expansions of the mapping functions about the periodic orbit:

$$p_1=f(p,q)=p_0+\frac{\partial f}{\partial p}(p-p_0)+\frac{\partial f}{\partial q}(q-q_0)+\frac{1}{2}\frac{\partial^2 f}{\partial p^2}(p-p_0)^2+\frac{\partial^2 f}{\partial p\partial q}(p-p_0)(q-q_0)+\frac{1}{2}\frac{\partial^2 f}{\partial q^2}(q-q_0)^2+\ldots \tag{3.7}$$

and similarly for $q_1=g(p,q)$. The first derivatives $\partial f/\partial p$, $\partial f/\partial q$, $\partial g/\partial p$, and $\partial g/\partial q$ determine the stability and the winding number or Lyapunov exponent of the orbit, and the second derivatives, provided that they do not vanish, determine the structure of the bifurcations. It would be "unusual" for the second derivatives to vanish at precisely the point at which the trace passes through 2.

However, if the map has a type of symmetry that is common in physics (though exceptional in function space), then the second derivatives vanish everywhere. In this case, the bifurcation structure is determined by the third derivatives. Different bifurcations occur in maps having such symmetries.

The Hamiltonian (2.5) possesses a periodic orbit $(u(t),p_u(t),v(t)=0,p_v(t)=0)$, and its orbits have the symmetries given by Eqs. (2.6). It follows that the Poincaré map (2.9) has the symmetry

$$\mathbf{f}(-\mathbf{z};\varepsilon)=-\mathbf{f}(\mathbf{z};\varepsilon)\ , \tag{3.8}$$

so all even-order derivatives vanish.

This symmetry modifies the structures of the bifurcations. The bifurcations of two-dimensional maps having the symmetry (3.8) are

m	Bifurcations
1	Pitchfork or antipitchfork
2	Standard period doubling
3	Doubled three-island chain bifurcation (symmetric period-tripling)
4	Touch-and-go or four-island chain bifurcation
5	$\geq m$-island chain bifurcation (m even) Doubled m-island chain bifurcation (m odd).

(3.9)

Properties of each of these bifurcations are discussed in Appendix B. (de Aguiar *et al.* [8(b)] studied bifurcations of orbits with symmetries, but they did not look at our case. Their potential energy has reflection symmetry in one variable, while ours has reflection symmetries in both variables.)

C. Linearization about a periodic orbit and Hill's equation

Consider again the orbit lying on the u axis: $(u(t), p_u(t), v(t)=0, p_v(t)=0)$. We take it to start at $u=0$ with $p_u>0$, and pass through $u=0$ with $p_u<0$ at $t=T_c$. If we regard this $u(t)$ as a given function, then we can obtain equations of motion for small displacements about this orbit

$$\frac{dv}{dt}=p_v\ ,\qquad \frac{dp_v}{dt}=-k(t)v\ , \tag{3.10a}$$

where

$$k(t)=\left.\frac{\partial^2 V(u,v)}{\partial v^2}\right|_{u=u(t),v=0} \tag{3.10b}$$

is a periodic function of time. Equation (3.10) is Hill's equation. It is an approximate equation for the transverse displacements about the periodic orbit $[u=u(t),v=0]$ when those displacements are small. This approximation does not conserve energy: the specified motion $u(t)$ drives $v(t)$ parametrically [through $k(t)$], but the effect of $v(t)$ on $u(t)$ is neglected.

Consider now an arbitrary small initial displacement $(p_v(0),v(0))$. Suppose we integrate Eqs. (3.10) through one-half cycle of the u motion, from $t=0$ to $t=T_c$, thus obtaining $(p_v(T_c),v(T_c))$. Since Eqs. (3.10) are linear, there is a linear relationship between initial and final variables, which we denote by

$$\begin{pmatrix} p_v(T_c) \\ v(T_c) \end{pmatrix}=\underline{J}_{\parallel}^{H}(\varepsilon)\begin{pmatrix} p_v(0) \\ v(0) \end{pmatrix}\ . \tag{3.11}$$

Intuitively, it is clear that $\underline{J}_{\parallel}^{H}(\varepsilon)$ has practically the same meaning as $\underline{J}_1(p_v^0=0,v^0=0;\varepsilon)$, and in fact we can prove that in this case the two matrices are identical,

$$\underline{J}_{\parallel}^{H}(\varepsilon)=\underline{J}_1(p_v^0=0,v^0=0;\varepsilon)\ . \tag{3.12}$$

It follows that Hill's equation can be used to calculate the trace of $\underline{J}_1$, and thereby to locate zones of stability and instability of the central orbit. Such calculations for the parallel orbit have been carried out by Edmonds [15]. (On the other hand, the actual structure of the bifurcations cannot be obtained from Hill's equation, because the structure depends upon nonlinear terms in the Hamiltonian; to obtain this information we must turn to Meyer's theorem and its modifications.)

Formulas for the trace of $\underline{J}_{\parallel}^{H}(\varepsilon)$ have been derived by Magnus and Winkler [16]. In our case, for the orbit along the magnetic field, the simplest approximation is

$$\mathrm{Tr}[\underline{J}_{\parallel}^{H}(\varepsilon)]=2\cos(w\pi)+[\pi/(2w)]\sin(w\pi)(w^2-1)\times(13w^2-61)/36(w^2-4)+\cdots\ , \tag{3.13}$$

where $w=[1+3/(-16\varepsilon^3)]^{1/2}$ is the winding number.

Hill's equation can also be applied to the perpendicular orbit; in that case we use a different surface of section

(defined in Sec. V), and we find that the lowest-order approximation to the relevant trace is

$$\mathrm{Tr}[\underline{J}_{\parallel}^{H}(\varepsilon)]=\begin{cases}2\cos(w'\pi)+\cdots\ , & w' \text{ real}\\ 2\cosh(|w'|\pi)+\cdots\ , & w' \text{ imaginary}\ ,\end{cases} \tag{3.14}$$

where $w'=[1+3/(64\varepsilon^3)]^{1/2}$.

Equations (3.13) and (3.14) are exact when carried to all orders; however, we found them to be rather slowly converging, so we used only the terms written to get simple approximations and we obtain the exact $\underline{J}_1(p_v^0,v^0;\varepsilon)$ by numerical integration of the exact equations of motion.

This concludes the general theory. In the following sections we present a series of "case studies." Each illustrates the unique character of a particular type of bifurcation. A few also show how two or more distinct bifurcations may be closely connected to each other. Together, the various cases illustrate the most important conclusion of this paper: Every bifurcation we have studied falls into one of the fundamental types listed above. A second important fact will be established in a later paper: almost every case discussed below is visible in the experiments [2].

IV. SADDLE-NODE BIFURCATIONS AND THE CREATION OF "EXOTIC" ORBITS

At a sufficiently low scaled energy, there exist only two simple orbits that are closed at the nucleus, one perpendicular to and the other parallel to the external magnetic field. When the scaled energy increases, more and more closed orbits appear. Most of them are associated with the two basic orbits: they are either directly created in bifurcations of the two basic orbits, or are created in further bifurcations of the resulting new orbits. In addition, a small portion of closed orbits are not associated with the two basic orbits: they are either created by saddle-node bifurcations, or are created in further bifurcations of the resulting orbits. In this section we examine saddle-node bifurcations.

Pictures of many of the orbits that we discuss in this paper are shown in Fig. 2. At the lower left corner of each picture, we give a label for it [17,18]. The label will

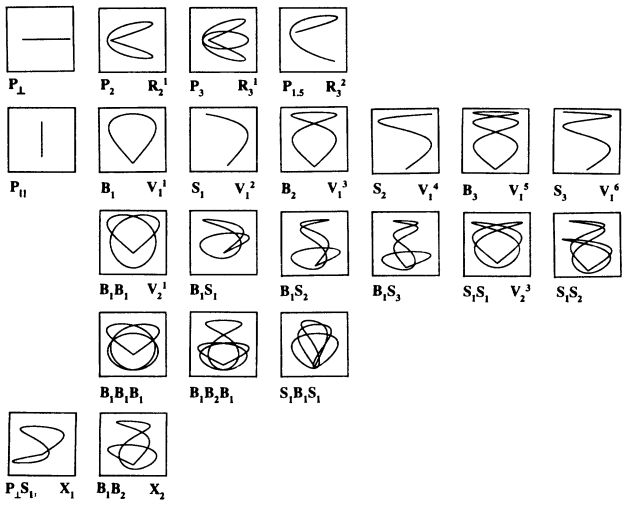

FIG. 2. Some electron orbits that are closed at the nucleus, in (ρ,z) space with z axis pointing up. The label in the lower left corner of each picture will be used in the text. The label in the lower right corner of each picture was used in Ref. [3(b)]

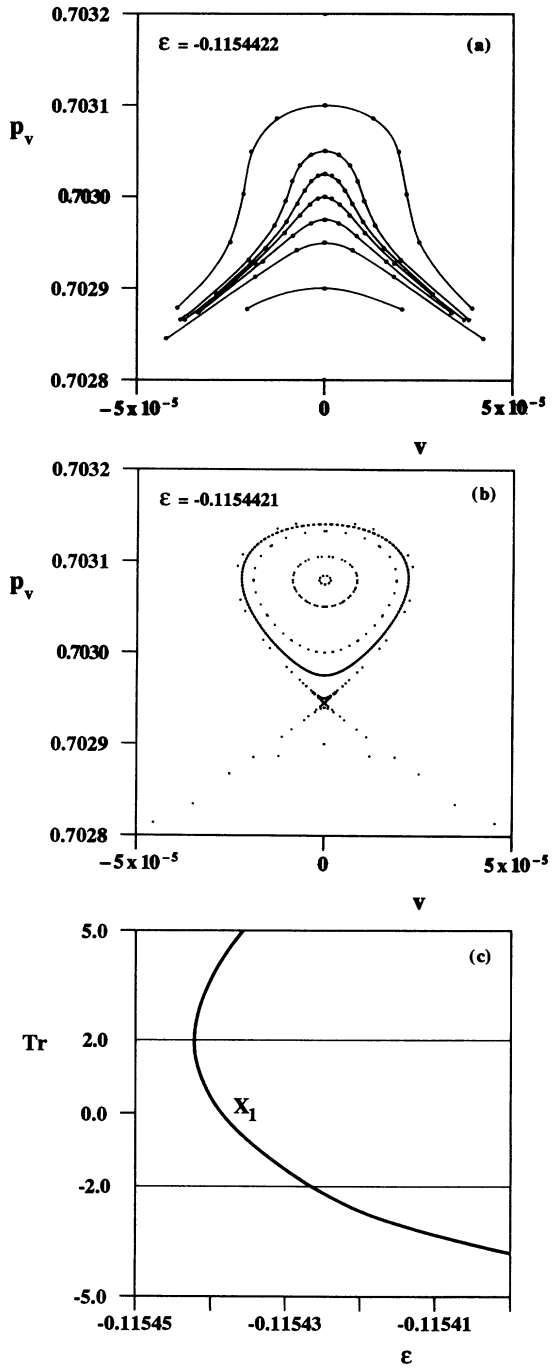

FIG. 3. A saddle-node bifurcation creates the "exotic" orbits X_1. Surface-of-section plots (a) for ε less than the critical value for the tangent bifurcation, and (b) for ε slightly greater than the critical value. (c) The ε dependence of the trace for the exotic orbits.

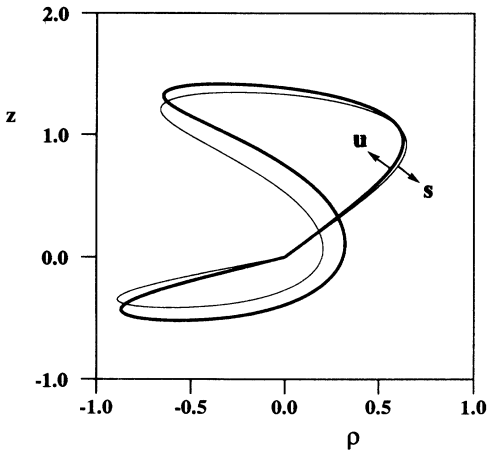

FIG. 4. The pair of exotic orbits X_1 created in the tangent bifurcation. One of them is stable and the other is unstable.

be used when the orbit is discussed in the text.

The orbits called "exotics" in Ref. [3] are created by saddle-node bifurcations (Appendix A). The simplest of these (called X_1 in Ref. [3]) is created at $\varepsilon=-0.115\,442\,16\ldots$, at which the trajectories are almost entirely chaotic. A surface-of-section plot will be shown later in Fig. 5(d) for $\varepsilon=-0.1$. If the seemingly chaotic region around $(v=0, p_v=0.703)$ is expanded by a factor of about 10^5, a tiny structure appears, shown in Figs. 3(a) and 3(b). (If the picture is turned upside down, one can see a v turn into a γ. Precisely at the bifurcation point one would see an Υ.) In Fig. 3(b) we see that a new stable and a new unstable periodic orbit have appeared "out of nowhere" [19]. Conversely, as ε decreases, an X point and an O point collide and annihilate. This structure is the signature of a Hamiltonian saddle-node bifurcation. A larger picture of the resulting orbits is shown in Fig. 4, with the stable and unstable member labeled s and u.

It may seem surprising that such a tiny structure in phase space can be visible in experiments. We will show in a future paper that the Bielefeld experiments are so sensitive to such phenomena that these orbits show up quite dramatically.

In Fig. 3(c) is shown the trace of the Jacobi matrix evaluated at the position of the two new periodic orbits of the map. It is, of course, greater than 2 at the unstable orbit and less than 2 at the stable orbit; the two branches of the trace approach 2.0 with a square-root behavior.

TABLE I. Critical values of scaled energy for saddle-node bifurcation of winding number m/k.

m/k	ε	New orbit	p_v
4/1	−0.115 442 16	$P_1S_1=X_1$	0.7030
4/1	−0.2045	$B_1B_2=X_2$	0.3234
3/1	−0.319 853	$S_1B_1S_1$	0.4063
4/1	−0.3173	P_2	1.245
6/1	−0.2215	$P_{1.5}$	1.186

More complex exotics are created at lower energies. The critical values for the bifurcations that create X_1 and X_2 are listed in the first two rows of Table I. Other saddle-node bifurcations in this table are combined with bifurcations of the perpendicular or the parallel orbit, and they will be discussed in the following sections.

V. BIFURCATION FROM THE PERPENDICULAR ORBIT

The perpendicular closed orbit is the one with $z=0$ ($+z$ axis is the direction of the external field), or equivalently, $u(t)=v(t)$ for all t. Hence the u motion is identical to the v motion. The orbit will be labeled $P_\perp$.

A. The surface of section

To take advantage of the symmetries, we use a different surface of section for studying bifurcations of this orbit. Defining

$$x=(1/\sqrt{2})(u+v)\ ,$$
$$y=-(1/\sqrt{2})(u-v)\ , \tag{5.1}$$

the appropriate surface of section is the $p_y y$ plane ($x=0$) and, as before, we include points every time the orbit passes through $x=0$ with either sign of p_x. Then the perpendicular orbit has period 1, it passes through the origin of the surface of section, and the symmetry (3.8) applies, so the bifurcations will be those given in Appendix B.

A few surface-of-section plots are shown in Fig. 5 for $\varepsilon=-1.0$, -0.4, -0.3, and -0.1. At low energy ($\varepsilon=-1.0$, for instance), there is no visible chaotic region. At medium energy, orderly and chaotic regions coexist, and for high energy ($\varepsilon=0$, for instance), there is no visible orderly region. Any fixed point on the p_y axis represents an orbit closed at the nucleus.

B. Stability

The linear stability of the perpendicular orbit is determined by the trace of the Jacobian matrix of the half map, evaluated at $(p_y,y)=(0,0)$. As stated earlier, we calculated this matrix by numerical integration of the exact equations of motion. [With $x=0$, we started from two points $(p_y,y)=(\delta,0)$ and $(p_y,y)=(0,\delta)$, where δ is a small number, and ended when the orbit passed through $x=0$ again.]

The result is shown in Fig. 6, together with the lowest-order Magnus-Winkler approximation (3.14). The latter is qualitatively but not quantitatively correct. (We repeat that the Magnus-Winkler formulas are exact when carried to all orders.)

As $\varepsilon\to-\infty$ the trace approaches -2 from above, and as ε increases, the trace increases monotonically. From the scaled-energy dependence of this trace, we can find the critical values of the parameter ε at which m bifurcations occur, according to Eqs. (3.5) and (3.6). These critical values are listed in Table II.

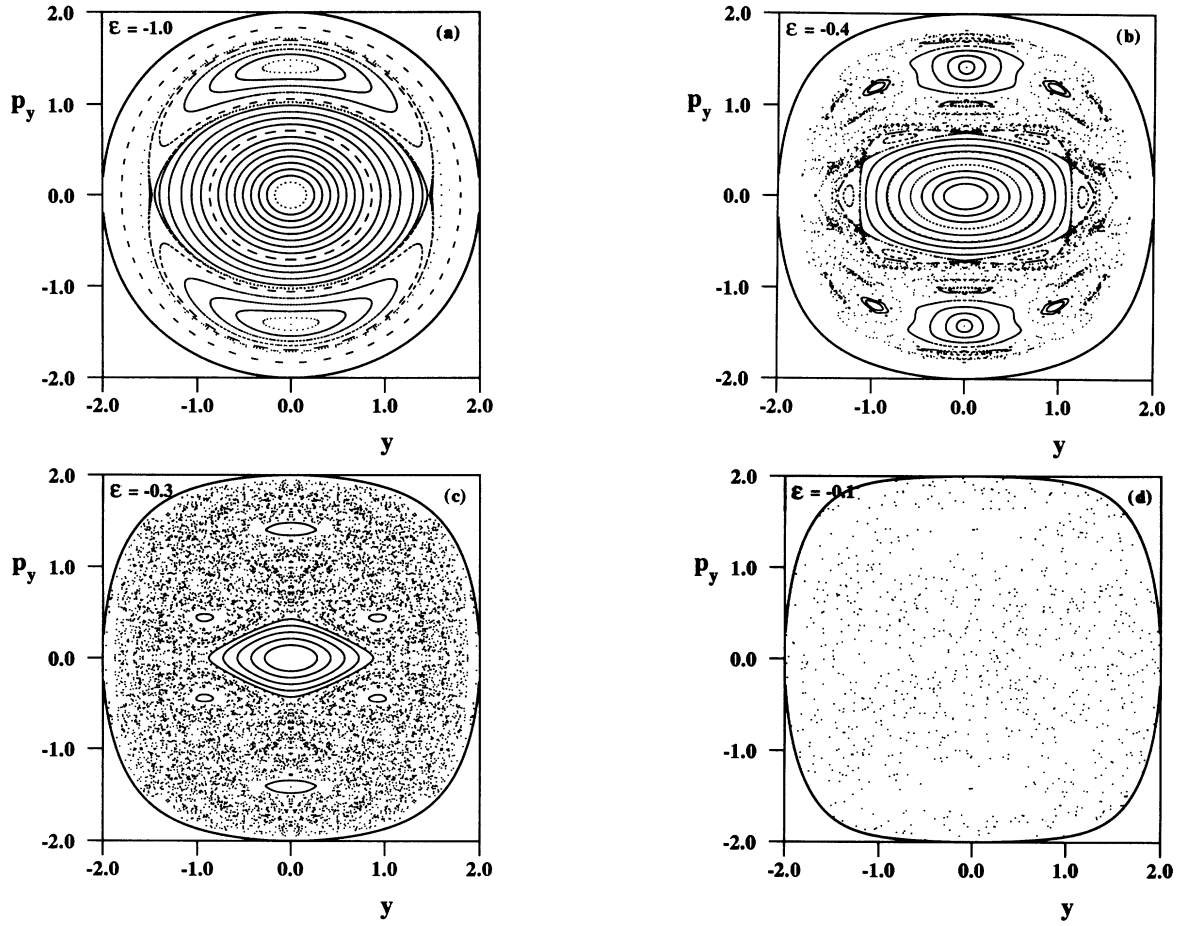

FIG. 5. Plots on the surface of section $x=0$ for (a) $\varepsilon=-1.0$, (b) $\varepsilon=-0.4$, (c) $\varepsilon=-0.3$, and (d) $\varepsilon=-0.1$.

C. Bifurcations

1. Period-1 bifurcation

The period-1 bifurcation occurs at $\varepsilon=-0.127\,268\ldots\equiv\varepsilon_1$, when the trace for the perpendicular orbit ($P_\perp$) equals 2. According to the classification for symmetric systems in Eq. (3.9), the period-1 bifurcation is either a pitchfork or antipitchfork bifurcation. It happens that the period-1 bifurcation of $P_\perp$ is an antipitchfork bifurcation: when ε increases, the stable perpendicular orbit becomes unstable and a pair of existing unstable orbits is destroyed. The destroyed orbits are shown in Fig. 7. They are not closed at the nucleus, so they are not relevant to present experiments. There is no period-2 bifurcation of $P_\perp$, because the trace never equals -2. (The trace tends to -2 when $\varepsilon\to-\infty$.)

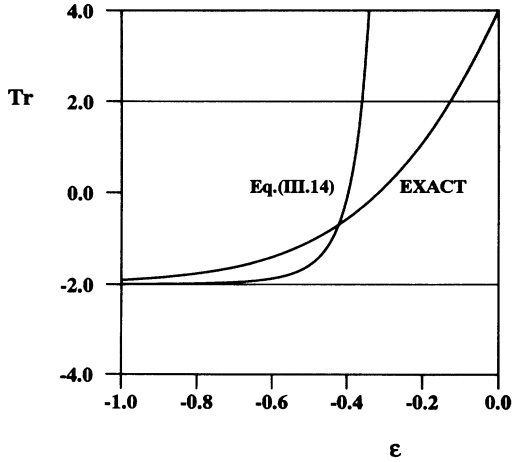

FIG. 6. The ε dependence of the trace for the perpendicular orbit. Both the exact result and the approximation given by Eq. (3.14) are shown.

2. Period-3 bifurcation

The period-3 bifurcation occurs when $\varepsilon=\varepsilon_3=-0.4828\ldots$ and $\mathrm{Tr}_1(0,\varepsilon_3)=-1$. According to Ap-

TABLE II. Critical values of scaled energy for m/k-bifurcation from the perpendicular orbit.

m/k	ε	New orbit
3/1	−0.4828	P_3
4/1	−0.3161	P_2
5/1	−0.2462	
5/2	−0.6972	
6/1	−0.2092	$P_{1.5}$

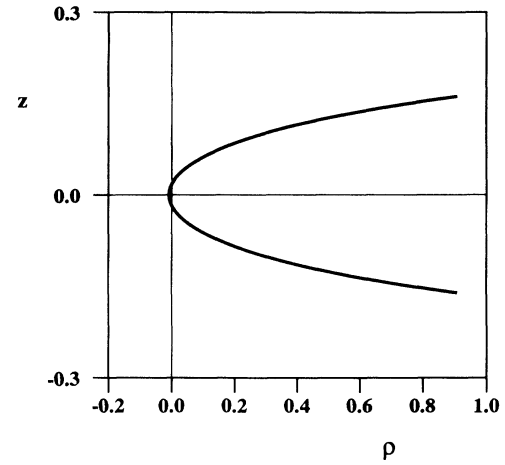

FIG. 7. The orbit destroyed at the period-1 antipitchfork bifurcation of the perpendicular orbit.

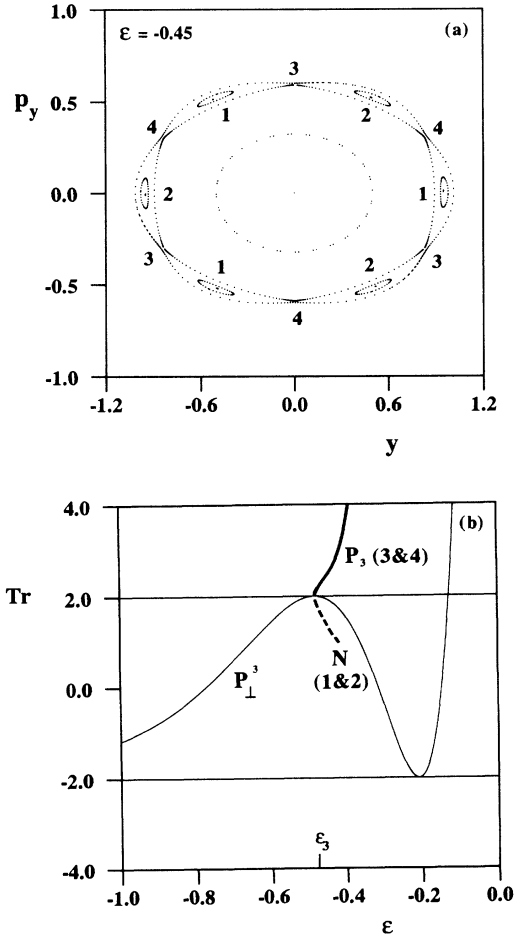

FIG. 8. The period-3 bifurcation of the perpendicular orbit. (a) The surface-of-section plot after the bifurcation. Four period-3 orbits labeled 1, 2, 3, and 4 are shown. (b) The ε dependence of the trace.

pendix B, we expect the creation or destruction of a double three-island chain: Two stable and two unstable period-3 orbits created simultaneously, while $P_\perp$ remains stable. Precisely this happens. The new periodic orbits are visible in the (p_y,y) surface of section shown in Fig. 8(a). They appear to form a chain of six islands, but actually they are two distinct chains of three islands labeled by (1,1,1) and (2,2,2) in Fig. 8(a). Only the two unstable orbits, labeled (3,3,3) and (4,4,4), have a point on the p_y axis ($y=0$) so only these touch the origin. On the surface of section, the X points are located symmetrically about the y axis, and it follows that one of the unstable orbits is the time reverse of the other. In contrast, the two new stable orbits are not connected by time-reversal symmetry, but by the reflection symmetry $z \rightarrow -z$.

The two new period-3 orbits that touch the nucleus are identical in (ρ,z) space, and they are shown in Fig. 2 under the label P_3. The other two have almost the same structure but they turn around near the nucleus without touching it.

Figure 8(b) shows $\mathrm{Tr}J_3(p_y,y;\varepsilon)$ evaluated at $P_\perp$ and at each of the newly created orbits. All the traces equal 2 at the bifurcation point, and as ε increases the trace at either unstable orbit increases while that at either stable orbit decreases. Since the orbits that are closed at the nucleus are unstable, they undergo no further bifurcations.

3. *The period-4 bifurcation and the creation of "Pacman"* $=P_2=R\frac{1}{2}$

The period-4 bifurcation should involve a four-island chain according to Appendix B. When ε passes through the critical value for the 4-bifurcation, $\varepsilon=\varepsilon_4=-0.3161\ldots$, where $\mathrm{Tr}_1(0,\varepsilon_4)=0$, a stable and an unstable period-4 orbit should be either created or annihilated. This prediction is correct, but much more happens as well.

At a lower energy, $\varepsilon\approx-0.325$, a saddle-node bifurcation occurs in the 4-map, and it creates a stable and an unstable orbit of period 4, labeled (1,1,1,1) and (2,2,2,2) in Fig. 9(a). When the energy is increased to $\varepsilon=\varepsilon_4^T=-0.3173\ldots$, a second saddle-node bifurcation occurs in the 4-map, creating the pair labeled (3,3,3,3) and (4,4,4,4) in Fig. 9(b). The X point and the O point associated with this saddle-node bifurcation both lie on the p_y axis, and only these two orbits touch the nucleus. They are shown in Fig. 10. We call either of these orbits "Pacman," after the creature in the computer game. (The other two orbits have almost the same shape, but they do not touch the nucleus.)

As ε increases, the stable and unstable orbits 1 and 2 move apart, as do 3 and 4. Then something unexpected happens. The separatrices of the X points 1 had been connected to each other, with a loop around the O points 2. Those of the X points 4 had been connected by a loop around 3. This topology was created by the saddle-node bifurcations. As the energy is increased, these separatrices collide and combine, and then disconnect in a different topology. In Fig. 9(c) we see that the separatrices from X points 1 now loop around O points 3, forming a four-island chain. The separatrices from X points 4

loop around O points 2 forming a second, larger island chain.

Further increasing the energy, the island chains move apart, with the smaller chain 1 and 3 approaching the origin. Finally at $\varepsilon=\varepsilon_4$ this chain collides with the origin and is annihilated, consistent with the prediction: a four-island chain disappears. In (ρ,z) space, the stable orbit moves to 90° and is annihilated (Fig. 10).

Orbits 2 and 4 persist to high energies, and the existence of orbit 4 has significant consequences in experiments. Since it is unstable, it has no further bifurcations. Figure 9(d) shows the scaled-energy dependence of the trace for all periodic orbits of the map shown in Fig. 9(b).

4. A 6-bifurcation

As an example of m bifurcations with $m \geq 5$, we have studied the 6-bifurcation. It should create or destroy a six-island chain, as indicated by Eq. (3.9). This case turns out to have the same complexity as the 4-bifurcation, and the structure is more clearly visible. At a low energy, a tangent bifurcation in the 6-map creates a stable and unstable pair [Fig. 11(a)]. Increasing the energy, a second tangent bifurcation creates another stable and unstable pair [Fig. 11(b)]. Further increasing the energy, the separatrices collide, and then disconnect with a new topology forming two six-island chains. The inner chain moves to the origin and is destroyed. The outer one moves away.

The surviving orbit, which is closed at the nucleus, is labeled $P_{1.5}$ in Fig. 2. It is stable, so it undergoes further bifurcations, but we do not discuss them here.

VI. BIFURCATIONS FROM THE PARALLEL ORBIT

The parallel orbit is the orbit along the direction of the external field (z axis). Bifurcations of this orbit produce the "main sequence" first discovered in Ref. [3]. These bifurcations have also been examined by Edmonds and by Wintgen [20] and others. Here we show how these bifurcations fit into the structures predicted in Appendix B, and how further bifurcations of the resulting orbits fit the predictions in Appendix A. In the uv plane, the parallel orbit is along the u axis or the v axis, cf. Eq. (2.4). The parallel orbit along the u axis ($v\equiv 0, p_v\equiv 0$) is represented by the origin of the vp_v plane, the Poincaré surface of section at $u=0$. The orbit along the v axis ($u\equiv 0, p_u\equiv 0$) represents the outer boundary of the surface of section.

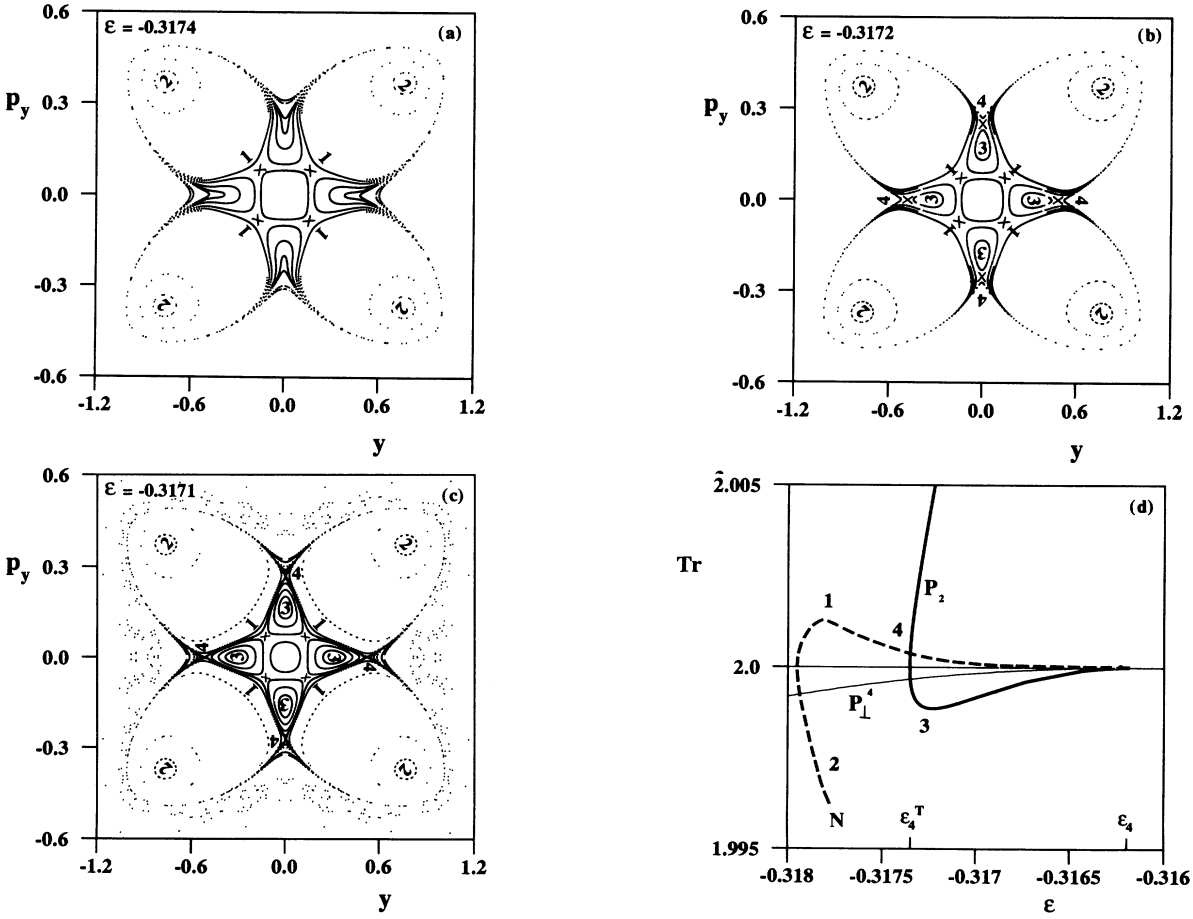

FIG. 9. The creation of "Pacman" orbits. A plot on the surface of section (a) after the first saddle-node bifurcation has occurred (the orbits 1 and 2 are not closed at the nucleus), (b) after the second saddle-node bifurcation has occurred (the orbits 3 and 4 are closed at the nucleus and are called Pacman orbits), and (c) after the separatrices have collided and reconnected. (d) The ε dependences of the trace for all orbits in (b). The curves 1 and 2 are not quantitative.

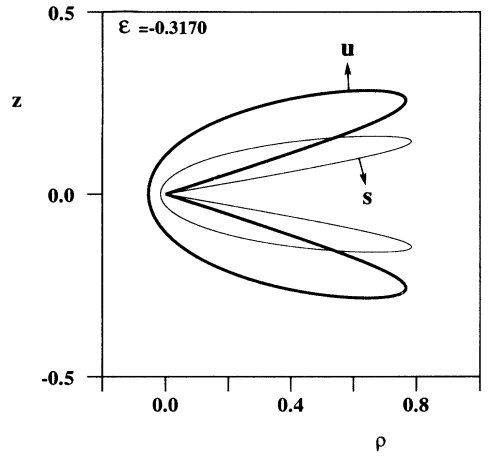

FIG. 10. The stable-unstable pair of "Pacmen" in (ρ,z) space.

A. Stability

As for the perpendicular orbit, we have numerically determined the Jacobian matrix of the half-map on the surface of section at $u=0$, evaluated at $p_v=v=0$, and its trace. Its dependence on scaled energy is shown in Fig. 12(a) as the thin oscillating curve labeled $P_{\|}$. From this dependence, the critical values of the scaled energy for m bifurcation can be determined according to Eq. (3.6). These critical values are listed in Table III.

The scaled-energy dependence of the trace can also be obtained by applying the Magnus-Winkler formulas. Again we found the simplest approximation (3.13) to be qualitatively but not quantitatively correct.

B. Bifurcations of the parallel orbit

The Hamiltonian (2.5) consists of only even powers of u, v, p_u, or p_v. Therefore, the surface-of-section plot in the $p_v v$ plane is symmetric about the v and p_v axes, and bifurcations of the parallel orbit should be that for symmetric systems, as listed in Appendix B.

1. Period-1 bifurcations

Period-1 bifurcations occur when the trace of the Jacobian matrix evaluated at $p_v=v=0$ reaches 2. This happens at points labeled B_i and N_i in Fig. 12(a). As indicat-

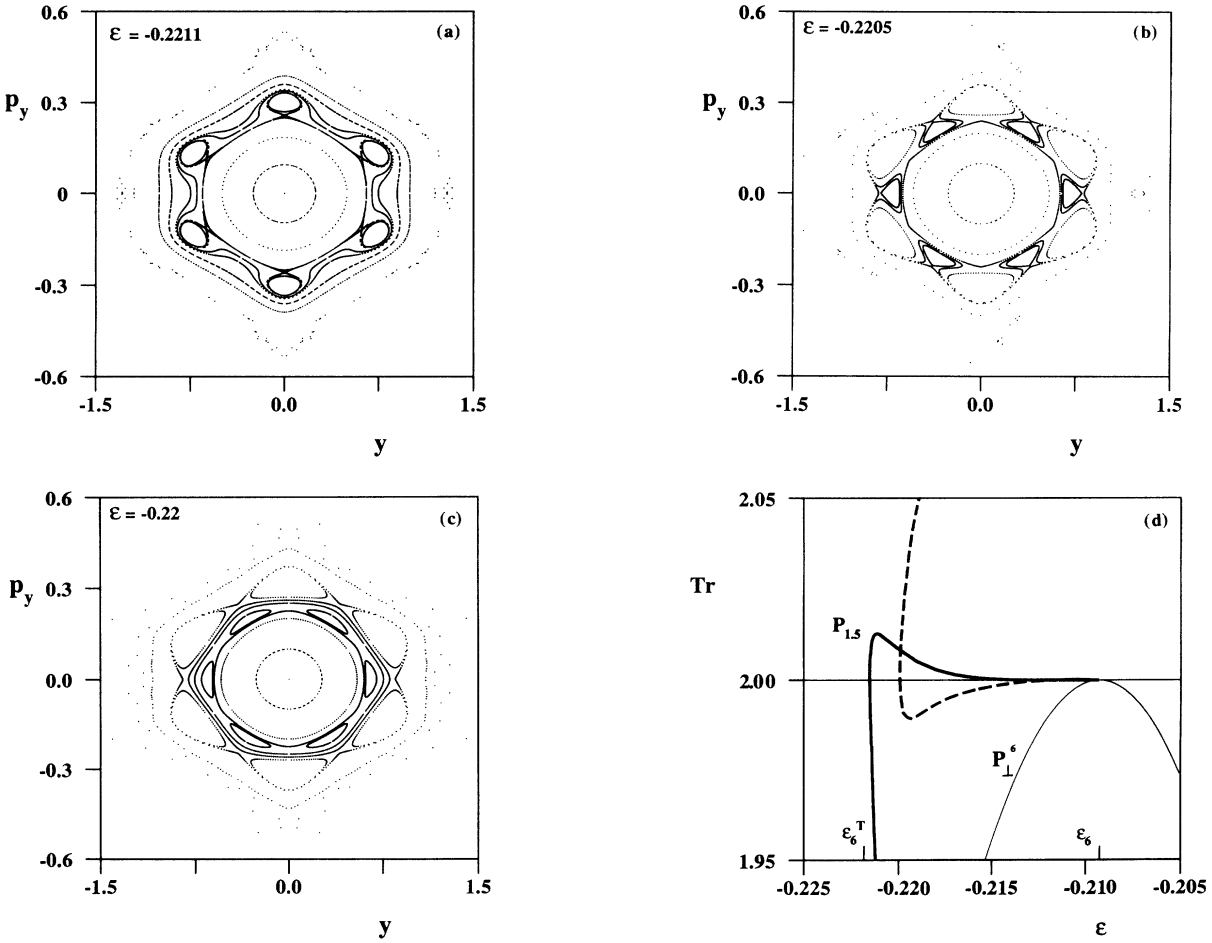

FIG. 11. The 6-bifurcations of the perpendicular orbit. A plot on the surface of section (a) after the first tangent bifurcation has occurred, (b) after the second tangent bifurcation has occurred, and (c) after the separatrices have collided and reconnected. (d) The ε dependences of the trace for all orbits in (b).

ed in Appendix B, the bifurcations should be either pitchfork or antipitchfork bifurcations.

At points labeled $(B_1,B_2,\ldots)$ a pitchfork bifurcation occurs: the parallel orbit becomes unstable, and a pair of stable periodic orbits of the same period is created. One member of the pair is the time reverse of the other. The trace curves for the newly created orbits are shown in bold in Fig. 12(a). The first of such bifurcations occurs at $\varepsilon=-0.3913\ldots$, at which the "balloon" orbit is created. The bifurcation is shown in Fig. 13.

TABLE III. Critical values of scaled energy for m/k-bifurcation from the parallel orbit.

m/k	ε	New orbit
1/1	−0.391 300 82	B_1
1/1	−0.215 382 86	B_2
1/1	−0.159 135 30	B_3
1/1	−0.129 497 70	B_4
1/1	−0.110 708 16	B_5
1/1	−0.097 539 41	B_6
1/1	−0.087 704 38	B_7
1/1	−0.080 028 26	B_8
1/1	−0.073 839 87	B_9
2/1	−0.270 987 97	S_1
2/1	−0.181 931 12	S_2
2/1	−0.142 403 70	S_3
2/1	−0.119 180 76	S_4
2/1	−0.103 601 84	S_5
2/1	−0.092 294 82	S_6
2/1	−0.083 646 38	S_7
2/1	−0.076 778 29	S_8
2/1	−0.071 167 77	S_9
3/1	−0.567 121 08	$B_1B_1B_1$
3/1	−0.283 078 90	
3/1	−0.232 443 09	
3/1	−0.185 424 53	
3/1	−0.165 914 34	
3/1	−0.144 117 60	
4/1	−0.486 433 92	B_1B_1
4/1	−0.294 569 96	
4/1	−0.226 597 90	S_1S_1
4/1	−0.188 638 47	
4/1	−0.163 658 49	
4/1	−0.145 689 37	
5/1	−0.453 764 39	
5/1	−0.302 380 23	
5/1	−0.223 260 60	
5/1	−0.190 687 75	
5/1	−0.162 325 67	
5/2	−0.684 021 76	
5/2	−0.275 886 68	
5/2	−0.236 772 24	
5/2	−0.183 341 51	
5/2	−0.167 490 47	
6/1	−0.436 158 56	$B_1S_1B_1$
6/1	−0.307 821 10	
6/1	−0.221 203 80	
6/1	−0.192 033 71	
6/1	−0.161 493 88	
6/1	−0.147 313 73	
	Bifurcations from $B1$ orbit	
3/1	−0.3184	$S_1B_1S_1$
4/1	−0.3425	B_1S_1

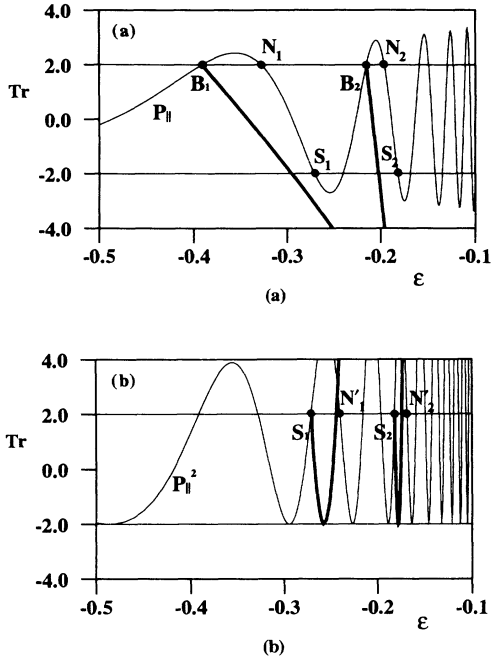

FIG. 12. Bifurcations of the parallel orbit. The thinner oscillating curves are the ε dependence of the trace for the parallel orbit. The bold curves are for the newly created orbits: balloon orbits (B_i) and snake orbits (S_i). N_i and N_i' denote the orbits that are not closed at the nucleus. (a) Creation of B_i orbits by pitchfork bifurcations. (b) Creation of S_i orbits by period-doubling bifurcations (pitchfork bifurcations in the 2-map).

At points labeled $N_1N_2,\ldots$, we have observed reversed antipitchfork bifurcations: the unstable parallel orbit becomes stable and a pair of unstable orbits is created. The new orbits do not close at the origin and therefore do not directly affect current experiments.

2. *Period-2 bifurcations*

Period-2 bifurcations occur when $\mathrm{Tr}_1(0;\varepsilon)=-2$, so $\mathrm{Tr}_2(0,\varepsilon)=2$. The dependence of $\mathrm{Tr}_2(0;\varepsilon)$ on the scaled energy is shown as the thin curve labeled by $P_{\|}^2$ in Fig. 12(b). The trace curves for the new orbits are in bold. The trace curve for $P_{\|}^2$ reaches 2 at points S_i and N_i' in the figure, in addition to the points that are also intersection points of the trace curve for $P_{\|}$ with the line $\mathrm{Tr}=2$. At points S_i, a pair of stable period-2 orbits is created. Each orbit is the reflection of the other. At points N_i', a pair of unstable period-2 orbits is created. The orbits are not closed at the nucleus. Hence, consistent with Appendix B, the bifurcations at points S_i and N_i' are each one of the two types of period doubling.

The set of orbits B_i and S_i produced by pitchfork and period doubling constitute the main sequence [3]. The

parallel orbit also gives higher-period bifurcations, which we discuss below.

3. *Higher-period bifurcations*

Bifurcations of period 3 or higher should be all be island-chain type because of the symmetries of the system. Unlike the bifurcations of the perpendicular orbit, these are *not* connected to nearby tangent bifurcations.

For period-m (m odd) bifurcations, such as period-3,-5,. . . bifurcations, four period-m orbits are created. Two of them are closed at the nucleus and two are not. The two that pass through the nucleus are either both stable or both unstable.

The 3-bifurcation with lowest scaled energy occurs at $\varepsilon=-0.567\,121\,08\ldots$, in which a pair of period-3 stable closed orbits is created. The surface of section is analogous to that shown in Fig. 8, except that in this case the O points (stable orbits) lie on the p_v axis. Their trajectories in ρz space are labeled $B_1B_1B_1$ in Fig. 2.

For period-m (m even) bifurcations, two new orbits are created, one stable and one unstable, one closed at the nucleus and one not. The 4-bifurcation with the lowest scaled energy occurs at $\varepsilon=-0.486\,433\,92\ldots$, and it produces the orbit labeled B_1B_1 in Fig. 2. Similarly, the other 4-bifurcations at the other critical values of scaled energy create closed orbits S_1S_1 or $B_2B_2,\ldots$. The 6-bifurcation with the lowest scaled energy creates the closed orbit labeled $B_1S_1B_1$ in Fig. 2.

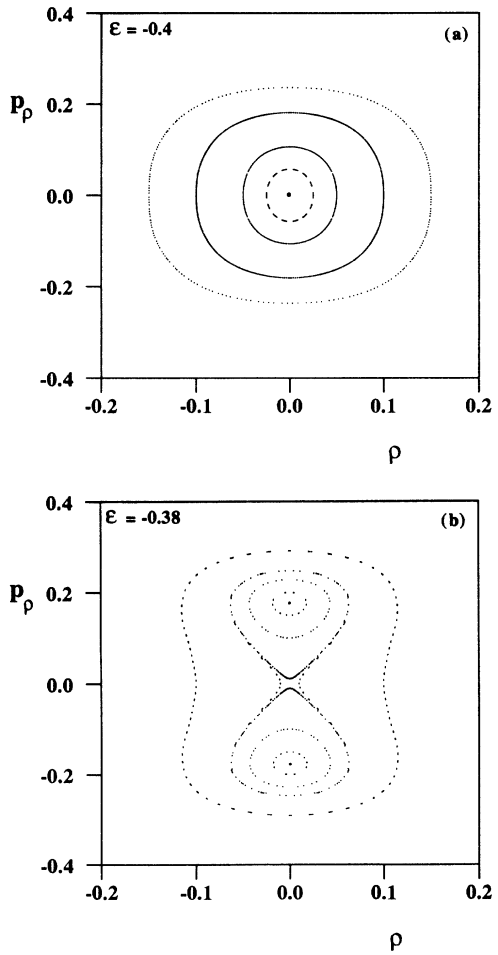

FIG. 13. Pitchfork bifurcation: the creation of "balloon" orbit B_1. A plot on the surface of section (a) before the bifurcation, and (b) after the bifurcation.

VII. BIFURCATIONS OF THE BALLOON ORBIT

The orbits B_i and S_i in the main sequence are stable when they are created, so they have the possibility of further bifurcations. These orbits are represented by points on the p_v axis of the surface of section. Since they are not at the origin, the symmetry (3.8) does not apply, and their bifurcations are those of generic systems, as discussed in Appendix A. The odd-order bifurcations should therefore have different structures from those discussed above. As an example, we examine some bifurcations of the balloon orbit.

Period-2 bifurcations of the balloonlike orbits are antipitchfork bifurcations: a pair of unstable orbits annihilate at the bifurcation point. It happens that the disappearing orbits are not closed at the origin.

Period-3 bifurcation from B_1 is interesting because maps lacking the symmetry (3.8) normally will not give trifurcations. The period-3 resonance is combined with a nearby saddle-node bifurcation, and a "touch-and-go" bifurcation occurs at the critical ε.

Specifically, at $\varepsilon=\varepsilon_3^T(B_1)=-0.319\,853\ldots$, a pair of period-3 orbits are created by saddle-node bifurcation. Both new orbits are of similar shape, labeled $S_1B_1S_1$ in Fig. 2, and both are closed at the origin. One of them is stable, and the other is unstable. In Fig. 14(a) we see a set of three O points and we infer a nearby set of X points.

After their creation in this bifurcation, the two orbits move apart when ε increases. The three O points move away from the center of Fig. 14(a), and the X points move toward the center, where the O point corresponding to the balloon orbit is waiting. In ρz space, the unstable orbit gradually changes shape, until at $\varepsilon=\varepsilon_3(B_1)=-0.3184\ldots$, it becomes identical to the third repetition of the balloon orbit. At this value of ε the surface of section is shown in Fig. 14(b): the three X points and their separatrices have collided with the origin. The unstable orbit does not then disappear, but continues to exist at larger ε, as seen in Fig. 14(c). This is a characteristic touch-and-go bifurcation [21].

VIII. SUMMARY OF PRINCIPAL CONCLUSIONS

1. Bifurcations of periodic orbits are important because they produce effects that are visible in spectroscopic experiments.

2. For Hamiltonian systems with two degrees of freedom there are five generic types of bifurcation. These types may be modified by symmetries of the system.

3. Every bifurcation we have studied fits one of the five types. Specifically, (a) saddle-node bifurcations produce the "exotic" orbits; (b) pitchforks and period doublings produce the main sequence of "balloons" and "snakes" from the parallel orbit; (c) period-triplings, which occur

only under symmetric conditions, produce $B_1B_1B_1$ and P_3; (d) a combination of a saddle-node bifurcation together with a generic touch-and-go bifurcation produces $S_1B_1S_1$ from the balloon; (e) a sequence of two saddle-node bifurcations followed by destruction of a four-island chain produces "Pacman" orbits P_2; (f) creation of four-island chains produces B_1B_1, S_1S_1, and B_2B_2, and creation of a six-island chain produces $P_{1.5}$.

ACKNOWLEDGMENTS

We especially thank John Shaw for many hours of helpful discussions. One of us (J.M.M.) would like to express thanks to S. K. Knudson for allowing use of his computer programs, and for help in the use. We also thank G. T. Rublein for explaining to us some aspects of bifurcation theory. This work was supported by the Office of Naval Research, the National Science Foundation, and the Jeffress Foundation.

APPENDIX A: PROPERTIES OF GENERIC BIFURCATIONS

(1) *Saddle-node bifurcation* (also sometimes called a tangent bifurcation; in Hamiltonian systems a more proper name is saddle-center bifurcation). When the parameter ε reaches a critical value ε_1, a stable and an unstable periodic orbit suddenly appear simultaneously at a point z_1 at which $\mathrm{Tr}_m(z_1,\varepsilon_1)=2$. As ε varies, the two orbits move apart, and we denote their locations by $z_s(\varepsilon)$ and $z_u(\varepsilon)$ for the stable and unstable orbits, respectively. According to theorem (2) of Sec. III A, $z_s(\varepsilon)$ and $z_u(\varepsilon)$ are continuous functions of ε. However, at the bifurcation, as $\varepsilon\rightarrow\varepsilon_1$, $(d/d\varepsilon)|z_s(\varepsilon)-z_u(\varepsilon)|$ goes to infinity; i.e, the orbits initially move apart at an infinite rate. The trace evaluated at the stable one becomes less than 2, and the trace at the unstable one becomes greater than 2; at the bifurcation the trace also has an infinite derivative:

$$\lim\frac{d}{d\varepsilon}[\mathrm{Tr}_m(z_{s,u}(\varepsilon);\varepsilon)]\rightarrow\pm\infty\ , \tag{A1}$$

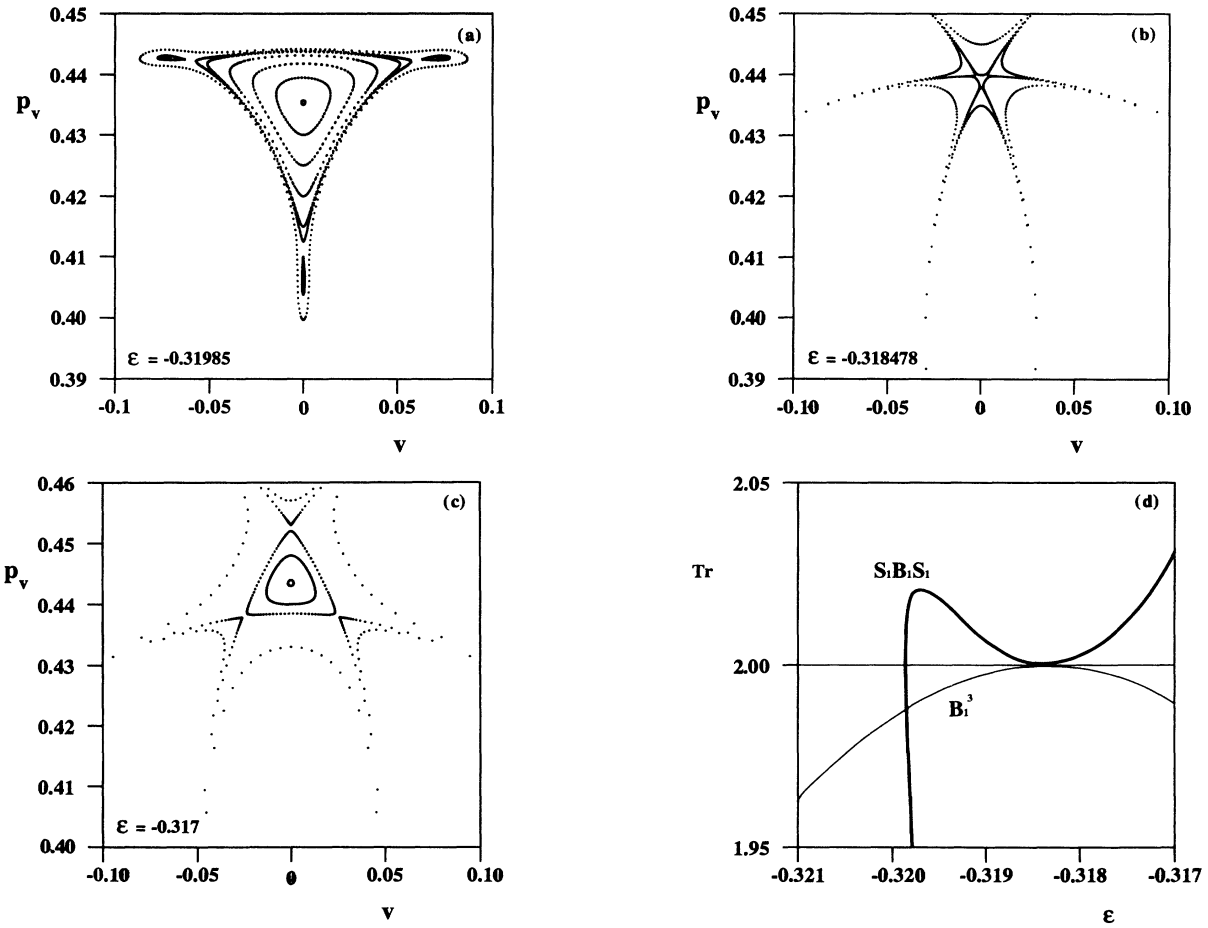

FIG. 14. Touch-and-go bifurcation: the 3-bifurcation of the B_1 orbit. (a) A plot on the surface of section before the bifurcation. B_1 is at the center of the large triangular island. A stable and unstable pair of period-3 orbits is created in a saddle-node bifurcation. (b) ε is very near the critical value for the bifurcation. The island of B_1 shrinks to the center, and the three X points also move into the same center. (c) After the bifurcation. The X points pass through the center, and the triangular island appears again but with the opposite orientation. (d) The ε dependences of the trace for the third repetition of B_1, and for the period-3 orbits $S_1B_1S_1$.

since $\mathrm{Tr}_m(\mathbf{z}_{s,u}(\varepsilon);\varepsilon)-2$ is proportional to $(\varepsilon-\varepsilon_1)^{1/2}$. We can also view the bifurcation by varying the parameter in the opposite direction: A pair of existing orbits, one stable and the other unstable, collide and disappear.

Saddle-node bifurcations are the typical way that new periodic orbits are created "out of nowhere" within a surface of section [8]. The remaining theorems describe how orbits may be created by bifurcation from an existing periodic orbit. We assume that over a range of ε there is an isolated period-m orbit of the map at a point $\mathbf{z}_0(\varepsilon)$, varying smoothly with ε.

(2) *Period doubling.* When $\mathrm{Tr}_m(\mathbf{z}_0(\varepsilon);\varepsilon)$ evaluated at an existing stable periodic orbit passes through -2 as the parameter ε varies, then that orbit becomes unstable, and either (a) a new stable orbit of period $2m$ appears, or (b) an existing unstable orbit of period $2m$ disappears. At the bifurcation, the two points of the new period-2 orbit on the surface of section move apart at an infinite rate as the parameter varies, but the derivative of the trace is finite and nonzero:

$$0<\left|\frac{d}{d\varepsilon}[\mathrm{Tr}_{2m}(\mathbf{z}_{s,u}(\varepsilon);\varepsilon)]\right|<\infty\ . \tag{A2}$$

Again, we can view the bifurcation by varying the parameter in the opposite direction. Period doubling can also be regarded as a "pitchfork" bifurcation of the $2m$-map (Appendix B).

(3) *Touch and go of period 3.* This occurs at a value of $\varepsilon=\varepsilon_3$ such that $\mathrm{Tr}_m(\mathbf{z}_0(\varepsilon),\varepsilon)$ passes through -1. At this point the existing orbit remains stable, and no new orbit is created. Instead, for ε near ε_3, surrounding $\mathbf{z}_0$ there is a small island of stability. Nearby there is an unstable orbit of period $3m$, at points labeled $\mathbf{z}_u^i(\varepsilon)$, $i=1,2,3$. The stable and unstable manifolds (separatrices) coming out of these three points bound the island of stability. As ε passes through ε_3, the three points of this unstable orbit pass through the stable orbit at a finite rate. The island of stability shrinks, disappears, and then reappears, with reversed orientation.

The trace has the following property: evaluated at the stable orbit, as stated above, $\mathrm{Tr}_m(\mathbf{z}_0(\varepsilon),\varepsilon)$ passes through -1 and $\mathrm{Tr}_{3m}(\mathbf{z}_0(\varepsilon),\varepsilon)$ grazes 2 from below. Evaluated at the unstable period-3 orbit, $\mathrm{Tr}_{3m}(\mathbf{z}_u^i(\varepsilon),\varepsilon)$ grazes 2 from above: at $\varepsilon=\varepsilon_3$,

$$\mathrm{Tr}_{3m}(\mathbf{z}_0(\varepsilon_3);\varepsilon_3)=\mathrm{Tr}_{3m}(\mathbf{z}_u^i(\varepsilon_3);\varepsilon_3)=2\ ,$$
$$\frac{d}{d\varepsilon}\mathrm{Tr}_{3m}(\mathbf{z}_0(\varepsilon),\varepsilon)|_{\varepsilon=\varepsilon_3}=\frac{d}{d\varepsilon}\mathrm{Tr}_{3m}(\mathbf{z}_u^i(\varepsilon_3),\varepsilon_3)|_{\varepsilon=\varepsilon_3}=0\ , \tag{A3}$$

This theorem makes no assertion about where the unstable 3-periodic orbit comes from, but it says that it is not born at the original periodic orbit. Typical two-dimensional area-preserving maps do not give period tripling. Our calculations show that such orbits are often created as tangent bifurcations of the 3-map: on the surface of section, three X points and three O points are created simultaneously. Then as ε varies, the X points migrate to the vicinity of a stable periodic orbit, where this touch-and-go bifurcation occurs.

(4) Two different types of period-4 bifurcation exist. One or the other occurs as $\mathrm{Tr}_m(\mathbf{z}_0(\varepsilon),\varepsilon)$ passes through zero.

(4a) *Touch and go of period 4* is very similar to that of period-3, except for the period. An unstable period-$4m$ orbit passes through the stable orbit at a finite rate.

(4b) *4-island chain bifurcation.* A pair of new period-$4m$ orbits, one stable and the other unstable, are created. In the surface of section, they form a chain around the period-m fixed point, and the chain consists of four islands separated by four hyperbolic fixed points. Alternatively, a period-$4m$ island chain collides with the stable orbit and is destroyed.

(5) *m-island chain bifurcation.* They are the same as the four-island chain bifurcation except for the number of islands, and the associated period, which is $5m, 6m, \ldots$.

APPENDIX B: BIFURCATIONS UNDER THE SYMMETRY (3.8)

At all values ε, the origin ($p=0, q=0$) is a fixed point of the map. We examine the bifurcations of this fixed point as the parameter ε varies.

(1) *Pitchfork bifurcation and antipitchfork bifurcation.* When $\mathrm{Tr}_1(\mathbf{0};\varepsilon)$ increases through $+2$, the orbit goes from stable to unstable, and either (a) a new pair of stable orbits with the same period appears (pitchfork bifurcation), or (b) a pair of existing unstable orbits with the same period disappears (antipitchfork bifurcation). Like the period doubling, the two orbits move apart (or together) at an infinite rate near the bifurcation, but in this case the derivative of the trace is finite,

$$\lim\frac{d}{d\varepsilon}[\mathrm{Tr}_m(\mathbf{z}_{s,u}(\varepsilon);\varepsilon)]\to\pm\infty\ ,$$
$$0<\left|\frac{d}{d\varepsilon}[\mathrm{Tr}_1(\mathbf{z}_{s,u}(\varepsilon;\varepsilon)]\right|<\infty\ . \tag{B1}$$

(2) *Period doubling.* This has been described in Appendix A. The symmetry does not change the structure.

(3) *Symmetric period tripling.* When the parameter reaches the critical value for the 3-bifurcation, four new orbits of period 3 are created, two of them stable, and the other two unstable. In the surface of section they appear to form a chain of six islands, but in fact they are two chains of three islands. The two stable orbits have the same trace for any given parameter value, and so do the pair of unstable orbits.

(4) *Four-island chain bifurcation.* This has been discussed in Appendix A.

(5) *m-island chain bifurcations for m even* are the same as those described in Appendix A. *Doubled m-island chain bifurcations* occur for m odd. They are analogous to the symmetric period tripling. Two m-island chains that have the appearance of a single $2m$-island chain are created or destroyed.

[1] W. R. S. Garton and F. S. Tomkins, Astrophys. J. **158**, 839 (1969); K. T. Lu, F. S. Tomkins, and W. R. S. Garton, Proc. R. Soc. London, Ser. A **362**, 421 (1978); A. R. Edmonds, J. Phys. (Paris) Colloq. **31**, C4-71 (1970).

[2] A. Holle, G. Wiebusch, J. Main, B. Hager, H. Rottke, and K. H. Welge, Phys. Rev. Lett. **56**, 2594 (1986).

[3] (a) J. Main, G. Wiebusch, A. Holle, and K. H. Welge, Phys. Rev. Lett. **57**, 2789 (1986); (b) A. Holle, J. Main, G. Wiebusch, H. Rottke, and K. H. Welge, *ibid.* **61**, 161 (1988).

[4] The argument is reproduced in E. A. Jackson, *Perspectives of Nonlinear Dynamics* (Cambridge University, Cambridge, England, 1989), Vol. 2, p. 41ff.

[5] M. L. Du and J. B. Delos, Phys. Rev. Lett. **58**, 1731 (1987); Phys. Rev. A **38**, 1896 (1988); **38**, 1913 (1988).

[6] N. Metropolis, M. L. Stein, and P. R. Stein, J. Combinatorial Theory **15**, (1), 25 (1973); M. J. Feigenbaum, J. Stat. Phys. **19**, 25 (1979); **21**, 669 (1979); P. Collet and J.-P. Eckmann, *Iterated Maps on the Interval as Dynamical Systems,* Progress in Physics Vol. 1 (Birkhauser-Verlag, Basel, 1980).

[7] J. Gleick, *Chaos: Making a New Science* (Viking, New York, 1987); E. A. Jackson, *Perspectives of Nonlinear Dynamics* (Cambridge University Press, Cambridge, England, 1989); A. J. Lichtenberg and M. A. Lieberman, *Regular and Stochastic Motion* (Springer-Verlag, New York, 1983); R.H.G. Helleman, in *Fundamental Problems in Statistical Mechanics,* edited by E. G. D. Cohen (North-Holland, Amsterdam, 1980), Vol. 5, p. 165; in *Long Time Prediction in Dynamics,* edited by W. Horton, L. Reichl, and V. Szebehely (Wiley, New York, 1982).

[8] (a) K. R. Meyer, Trans. Am. Math. Soc. **149**, 95 (1970); see also A. M. Ozorio de Almeida and M. Alfredo, *Hamiltonian Systems: Chaos and Quantization* (Cambridge University, Cambridge, England, 1988); (b) M. A. M. de Aguiar, C. P. Malta, M. Baranger, and K. T. R. Davies, Ann. Phys. **180**, 167 (1987). The symmetric case they studied is different from ours, so the special bifurcations they found are different from those described here.

[9] J. B. Delos, S. K. Knudson, and D. W. Noid, Phys. Rev. A **30**, 1208 (1984); R. Gajewski, Physica **47**, 575 (1970); M. Robnik, J. Phys. A **14**, 3195 (1981). The scaling transformation is written in Eq. (2.4) of the paper by J. B. Delos, S. K. Knudson, and D. W. Noid. The transformation used here differs from that one by a factor of 2 in the definition of r'. This makes the Hamiltonian identical to that used by Edmonds [15].

[10] E. L. Stiefel and G. Scheifele, *Linear and Regular Celestial Mechanics* (Springer-Verlag, New York, 1971); D. Wintgen and H. Friedrich, Phys. Rev. A **36**, 131 (1987); **35**, 1464 (1987).

[11] R. Abraham and J. E. Marsden, *Foundations of Mechanics* (Benjamin-Cummings, Reading, MA, 1978); D. Ruelle, *Elements of Differentiable Dynamics and Bifurcation Theory* (Academic, San Diego, 1989); J. Guckenheimar and P. Holmes, *Nonlinear Oscillations, Dynamical Systems, and Bifurcations of Vector Fields* (Springer-Verlag, New York, 1983).

[12] A trivial example is the two-dimensional anisotropic harmonic oscillator; it has two real periodic orbits at positive energy, and no real orbits at all at negative energy; the trace need not equal 2 at the boundary, $\varepsilon=0$.

[13] T. Poston and I. Stewart, *Catastrophe Theory and its Applications* (Pitman, London, 1978), especially p. 107ff.

[14] It follows that, for example, all typical one-dimensional oscillators are harmonic for small displacements; quartic oscillators exist, but they are rare—one would expect to find them only in systems with special symmetries.

[15] A. R. Edmonds, J. Phys. A **22**, L673 (1989).

[16] W. Magnus and S. Winkler, *Hill's Equation* (Interscience, New York, 1966).

[17] Our labels are quasidescriptive: B means balloon, S means snake, and P_k means Pacman with k lips. Combinations like B_1S_1 can be understood with some imagination. A more definitive labeling scheme was created by Eckhardt and Wintgen [18].

[18] B. Eckhardt and D. Wintgen, J. Phys. B **23**, 355 (1990).

[19] The new periodic orbits come "out of nowhere" because our dynamics is restricted to real values of coordinates and momenta. If the dynamics is extended to complex coordinates and momenta and the map (2.9) is analytic, then the new periodic orbits come down onto real coordinates from complex phase space.

[20] D. Wintgen, J. Phys. B **20**, L511 (1987).

[21] V. I. Arnold, *Mathematical Methods of Classical Mechanics* (Springer-Verlag, New York, 1978), p. 392.